DOI: 10.1002/ ((please add manuscript number))

Article type: Full Paper

Quantifying surface properties of silica particles by combining Hansen parameters and Reichardt's dye indicator data

Claudia Stauch, Sebastian Süß, Robert Luxenhofer, Bernard P. Binks, Doris Segets and Karl Mandel**

C. Stauch, Dr. K. Mandel
Fraunhofer Institute for Silicate Research ISC
Neunerplatz 2 D-97082, Würzburg, Germany
E-mail: karl.mandel@isc.fraunhofer.de
C. Stauch, Prof. R. Luxenhofer, Dr. K. Mandel
Chair of Chemical Technology of Materials Synthesis, Department Chemistry and Pharmacy
Julius-Maximilians-Universität Würzburg
Röntgenring 11, D-97070 Würzburg, Germany
S. Süß., Dr. S. Segets
Institute of Particle Technology, Friedrich-Alexander-Universität Erlangen-Nürnberg,
Cauerstr. 4, D-91058 Erlangen, Germany
E-Mail: doris.segets@fau.de
S. Süß
Interdisciplinary Center for Functional Particle Systems, Friedrich-Alexander-Universität Erlangen-Nürnberg
Haberstraße 9a, D-91058 Erlangen, Germany
Prof. B. Binks
School of Mathematics and Physical Sciences, University of Hull
Hull. HU6 7RX. UK

Keywords: colloidal stability, silica particles, interface characterization, surface coating, analytical centrifugation

To obtain quantitative understanding of the effects of a chemisorbed organic modification on the surface of particles, we discuss the use of Reichardt's dye (RD) and Hansen Solubility Parameter (HSP), whereby the S should be rather understood in terms of "similarity" rather than solubility as dispersibility is in focus. We chose silica nanoparticles modified to different extents with a medium chain silane including completely hydrophilic and hydrophobic particles. During spray drying, such particles form fully re-dispersible micro-raspberry superstructures. After qualitative estimations of the particles' polarity based on measuring both immersion time and ability of modified particles to stabilize oil-water emulsions, surface properties were quantified by HSP and RD. With increasing hydrophobicity, *i.e.* increasing amount of silane at the surface, all three contributions to HSP changed. At the same time, RD analysis revealed that the normalized solvent polarity parameter decreases progressively. HSP and RD analysis were in good agreement, giving strong confidence on each method applied individually. Our work demonstrates that after noticeable attempts for combined solubility parameters in case of molecules, carbon allotropes and gelators, such studies can be extended towards functional (nano)particles and that a holistic picture of particle surface properties is possible via the combination of different, quantitative techniques.

1. Introduction

Despite decades of progress in nanoparticle research, in particular the characterization of nanoparticle surfaces remains a major challenge today. For many applications, it is essential to modify nanoparticle surfaces with functional groups to render their compatibility with their environment, *e.g.* with polymer matrices in the case of polymer nanocomposite materials.[1–3] Nanoparticles in such polymers act as reinforcing fillers,[3–5] which play an important role in for example vehicle tyre technology. However, the well-controlled modification of nanoparticle surfaces is not only very beneficial for polymer composites, it is also crucial for

the stabilization of suspensions and emulsions.[6–8] For the latter, silica nanoparticles are particularly suitable to stabilize so-called Pickering emulsions.[9,10] The stability as well as the type of the formed emulsion (oil-in-water (o/w) or water-in-oil (o/w)) depends crucially on the polarity of the nanoparticles.[11–15]

To quantify the surface polarity of functional nanoparticles, advanced characterization is indispensable. Analytical techniques such as infrared spectroscopy or Raman spectroscopy are used to determine the presence of organic groups in general.[16,17] To quantify the amount of organic moieties in a nanoparticle sample, differential thermogravimetric analysis (TGA), ideally coupled to mass spectrometry, can be applied.[1,4] Furthermore, (solid state) nuclear magnetic resonance (NMR) spectroscopy is a powerful method, which is most often used to add information on the mode of bonding of molecules on nanoparticle surfaces,[18–21] although it should be noted that beyond obtaining only this, it was also demonstrated that NMR is capable of acting as a tool to quantify functional groups[22,23] or even to estimate particle size[24]. The combination of small angle X-ray and neutron scattering (SAXS/SANS) could become an important link between the molecular picture and wetting/dispersibility as it allows to analyze organic ligand shells around nanoparticles *in situ*.[25] However, such knowledge on surface chemistry on the molecular level cannot (yet) be linked to the particle level, *i.e.*, to predict the dispersibility of nanoparticles in different liquids. For technical formulation purposes, surface properties have to be described in terms of polarity measures. For instance, wettability measurements *via* drop contact angle techniques provide information on the degree of hydrophilicity/hydrophobicity of bulk surfaces. Unfortunately, such methods can only provide apparent information for nanoparticle surfaces since, besides geometrical constraints, particle roughness can also alter the contact angle of any droplet significantly.[26,27]

Thus, none of the above mentioned methods gives quantitative access to the degree of polarity of a surface of modified nanoparticles that can be compared *via* distinct numbers throughout different laboratories. Until now, only qualitative methods are applied for this purpose to obtain visual information of the polarity degree of modified particles by dispersing them in various liquids and assessing whether a stable dispersion forms or not.[28,29] To obtain well-defined nanocomposites or emulsions based on nanoparticles suitable for a certain application, only empirical knowledge and methods exist. Hence, for new nanoparticle classes, new methods are urgently needed to rationalize and predict whether stable nanoparticle dispersions can be successfully prepared or not. For practical applications, simple methods are desired to describe the degree of polarity of a particle system.

On the other hand, when looking on recent developments emerging from the field of molecules and molecule-like structures e.g. fullerenes,[30–32] polymers,[33,34] low molecular weight/mass gelators,[35–37] and resins,[38,39] it becomes clear that in particular the combination of different solubility parameters is desirable for getting the full picture. In most detail, Lan et al.[35,36] exercised that by an impressing study where up to 22 different solubility parameters were compared with each other. They found that solubility parameters could not accurately predict the gelation behavior of molecular gels (1,3:2,4-dibenzylidene sorbitol was used as model gelator) unless they could specifically address the ability of hydrogen bonding. Thus, Kamlet-Taft parameters as an extension of $E_T(30)$ and HSP were found to provide good correlations while global measures like partition coefficients and dipole moments did not.[36] Moreover, the authors pointed towards the use of multivariate statistical analyses to identify logical approaches for solvent classification as well as to pinpoint synergistic parameter combinations. However, this is certainly only possible when the determination of individual solubility parameters and their relationship to each other is sufficiently understood. For the time being, for nanoparticles this is certainly not the case.

Also worth mentioning are recently reported advanced mathematical approaches to compute HSP. Groups of Boucher and Howell developed a concept where so-called Convex Solubility Parameters (CSP) were introduced.[32] These overcome the need of spherical solubility regions using the convex hull of all good solvents with the CSP of interest being their focal point. In a follow up study the concept was extended towards Functional Solubility Parameters (FSP),[31] where a solubility function gives quantitative access to different levels of solubility. Similar to the approach used in here but mathematically more complicated and not (yet) established for nanoparticles, FPS are replacing the need of arbitrary 0/1 scoring into either good or poor.

Herein, we demonstrate how the combination of two quantitative methods for surface modified inorganic nanoparticles, namely Hansen parameters and Reichardts Dye (RD) can be combined with each other and how studying both approaches enables a mutual validation of each individual approach. To show the strength of this combination for the resolution of surface functionalities, we chose so-called nanostructured silica-based micro-raspberry particles as an interesting model system. It can be tuned over a wide range of polarity and obtained by spray-drying in large quantity with the resulting micron sized powder composed of modified nanoparticles being easy to handle and readily re-dispersible by mechanical activation.[40]

2. Surface property quantification

Hansen Parameters. A frequently used approach to assess the compatibility between different molecular compounds, in particular polymers and solvents, is the so-called Hansen Solubility Parameter (HSP).[41] Historically, Hansen divided another solubility parameter, the Hildebrandt parameter (HP), which goes back to the energy of vaporization and thus to the integral amount of all interactions within a molecule, into three parts. These are dispersion

interactions δ_D, describing the contribution of non-polar London interactions, polar interactions δ_P, describing the interactions of two permanent dipoles and hydrogen bonds δ_H, accounting for the ability of electron exchange based on the acid and base concept of Lewis. This allows creation of a three dimensional (3D) parameter space with three distinct coordinates. Then, like in any approach dealing with solubility parameters, HSP are based on the paradigm "like dissolves like", *i.e.* the solubility of the substance of interest is investigated in a defined set of probe liquids with known HSP. Thus, by challenging the target molecule in question with different probe liquids with known HSP coordinates and distinguishing them into "good" (dissolves the target molecule) and "poor" (does not dissolve the target molecule), solubility regions within the 3D interaction space are identified. Finally, by drawing a sphere around all "good probe liquids", the center of the sphere gives the HSP of the unknown target molecule. Once determined, suitable solvents are identified based on their HSP coordinates. The closer the HSP of the chosen solvent and the examined compound, the higher the solubility and *vice versa*.

In principle, as shown by others and Süß *et al.*,[42–50] the approach is transferable to (nano)particles although at this point it has to be mentioned that when moving from molecules to disperse systems, a boundary is crossed. Particulates are usually thermodynamically unstable because of the inherent phase boundary, *i.e.*, interface. Only for distinct cases of small nanoparticles with hard sphere behaviour the integral Gibbs energy of solvation can become < 0 kT.[51] Hence, as the thermodynamic basis of HP is left when transferring the approach to colloidal systems, the term Hansen Dispersibility Parameter (HDP) was suggested whenever particles are discussed,[47] or, at least the S in Hansen Solubility Parameter (HSP), should be understood in terms of "similarity" instead of solubility.[52]

Regarding the measurement of nanoparticles, Süß et al.[47] introduced recently a new, completely objective determination of HSP which makes the introduction of – inevitably

subjective – 0/1 scoring into either good or poor obsolete.[53] In brief, a standardized measurement and evaluation procedure for discrimination of probe liquids into "good" (*i.e.* is a suitable dispersion medium) and "poor" (*i.e.* is not a suitable dispersion medium) was developed using analytical centrifugation (AC) and an algorithm that is based on the step-wise switch on of good liquids. Validation was done by predicting the dispersibility of carbon black in untested liquids and liquid mixtures. Thus, by combining HDP with a standardized determination procedure, the surface properties of particles become quantitative accessible by distinct values of δ_D, δ_P and δ_H in an easy and accurate way.[47] Once determined properly, these could be potentially linked to the previously discussed surface chemistry on the molecular level allowing to address formulation as the true multiscale issue it is. Although this is highly challenging, recent developments on intensely studied model systems like ZnO do give some hope that this can be realized.[54–60]

Reichardt's Dye. For liquids, another method to determine polarity exists, namely the employment of solvatochromic indicators.[61–64] The working principle is as follows: The indicator, usually a dye, changes its color depending on the polarity of its immediate molecular environment. The solvatochromic effect which is for some dyes still in the focus of nowadays research,[65,66] can occur in two different ways, either as negative solvatochromism where a hypsochromic shift (blue shift) can be observed with increasing polarity, or as positive solvatochromism with a bathochromic shift (red shift). A widely used indicator is Reichardt's dye, RD (Figure S1a). RD exhibits a medium-dependent charge transfer transition in the visible region of the light spectrum. Polar liquids like methanol (MeOH) stabilize the molecular electronic ground state more than the excited state leading to an increased transition energy.[67] The RD exhibits one of the largest known negative solvatochromic effects (a blue shift with increasing polarity). The color of this dye ranges from green in non-polar liquids (acetone) to red in polar liquids (methanol) (Figure S1b). This color shift was used to create

the empirical liquid polarity parameter, $E_T(30)$. $E_T(30)$ is defined as the molar electronic transition energy of the betaine dye 30 in accordance with the longest-wavelength UV/Vis absorption maximum of RD under standard conditions (equation 1).[67] For a much easier handling, the normalized E_T^N value was introduced (equation 2).[67] Herein, tetramethylsilane (TMS) (E_T(TMS) = 30.7) was used as an extreme non-polar reference liquid and water (E_T(water) = 63.1) was used as the extreme polar reference liquid. With these limits the polarity scale ranges from 0 for TMS to 1 for water.

$$E_T(30)/\text{kcal mol}^{-1} = hc\tilde{\nu}_{max}N_A = (2.8591 \times 10^{-3})\ \tilde{\nu}_{max}\ (\text{cm}^{-1}) = 28591/\lambda_{max}\ (\text{nm}) \quad (1)$$

$$E_T^N = \frac{E_T(solvent) - E_T(TMS)}{E_T(water) - E_T(TMS)} = \frac{E_T(solvent) - 30.7}{32.4} \quad (2)$$

[1] h is Planck constant, c is the speed of light, N_A is Avogadro constant, $\tilde{\nu}_{max}$ is the frequency and λ_{max} the wavelength of the maximum of the longest wavelength, intramolecular charge transfer π-π*absorption band of RD

In fact, RD was already further developed from molecules to determine the surface polarity of particles,[68–72] but it is still far from being a standard method for the general characterization of particles, especially for particles with different modification degrees. Thus, proving its applicability to complex nanoparticles and comparing the results to another, independent technique, is seen as a major step forward in accessing particulate surface properties.

Micro-raspberry particles as model system. The idea of using the silica micro-raspberries was to create a nanoparticle system with adjustable properties which is very easy to handle and could be used for different applications. Starting with silica nanoparticles in suspension the particles were modified with silane and afterwards spray-dried to an easy to handle powder (Figure S2). This system is ideal to study the characterization potential of a combined HDP and RD analysis: Starting with the surface modification at single nanoparticle level, the approach firstly allows for a careful tuning of the degree of silanisation on the nanoparticle surfaces. Secondly, the drying approach gives a powder at hand which makes studies of

dispersion behavior in different solvents easy. Without drying, one would always face the problem of remaining traces of solvents when particles are transferred from one solvent to another. Using a powder as starting point overcomes this problem. The silane modification prevents irreversible hard agglomeration as demonstrated earlier.[40] We chose silane octyltriethoxysilane (OCTEO) as ligand which is able to gradually change the polarity of the nanoparticle surfaces from hydrophilic to hydrophobic (with using increasing amounts of silane). Despite OCTEO being a rather "simple" surface modifying agent, it has a great impact on the later properties of the modified particles regarding dispersibility or reinforcement of a matrix such as in an elastomer composite.[73] Here, the octyl groups transform the hydrophilic Si-OH groups on the surface of the primary silica nanoparticles into hydrophobic, hydrocarbon covered surfaces. Thus, by controlling the degree of silane coverage, the polarity of the primary particles can be gradually adjusted.[40] It should be noted that this study was carried out using a triethoxysilane, despite being aware that these silanes might undergo mutual condensation among each other and to some extend might complicate the analyses and interpretation. However, we think that for application relevance, it is important to try to establish a holistic picture for nanoparticles modified with commonly used silanes. To the best of our knowledge, the overwhelming majority of research and also development and application is done with silanes which have three reactive groups (triethoxy or trimethoxy). Moreover, for the time being any particle surface is ill-defined due to the inherent complexity of multiple functionalities, (surface) ions and atoms and adsorbed solvent molecules which are all interacting i) amongst each other, ii) the particle core and iii) the continuous phase. Therefore, we selected such a well-explored silane for our studies and did not choose e.g. monoalkoxysilanes.

Herein, with the combination of HDP and RD, two approaches are at hand that potentially allow for a quantitative determination of the nanoparticles' surface polarity across different

laboratories. To the best of our knowledge this is the first time this was done for complex, spary dried particulates and could, ultimately and on the long-term run, pave the way for predictions on the dispersibility of nanoparticles in solvents or polymer matrices.

3. Results and Discussion

3.1 Strategy

In this work, an approach for characterizing the particulate surface properties of silica-based nanostructured micro-raspberry particles is developed by combining different analytic methods. Starting with simple characterization methods like FTIR and TG measurements, which can provide a first positive indication of surface modification in general, liquid tests follow. Then, to get a much deeper understanding of the surface modification of the particles, advanced methods like HDP and RD are considered in combination. Finally, these two methods are validated against each other to gain the best possible insights regarding the changes in surface properties upon modification.

3.2 Simple methods

Liquid tests

The degree of re-dispersibility strongly depends on the polarity of the nanoparticle surface and thus on the degree of silane modification relative to the type of liquid or matrix the particles are dispersed in. In this study, silica nanoparticles with different degrees of OCTEO surface modification (completely modified 1, partly modified 2/3, 1/2, 1/3, 1/5, 1/10 which means a reduction of the degree of modification down to 2/3, 1/2, 1/3, 1/5, 1/10 of the surface of the primary nanoparticles compared to completely modified and non-modified, *i.e.* 0) were used. The silane is hydrolyzed and can subsequently covalently bind to the silica surface *via* condensation. Qualitative evidence of silane on the nanoparticle surfaces was conducted by

FTIR measurements and reported before by Stauch *et al.* (Figure S3).[73] Compared to non-modified particles, new peaks between 3000 cm^{-1} and 2800 cm^{-1} were found for modified particles, which can be assigned to the CH_2- and CH_3- stretching modes from the OCTEO molecules bound to the silica surface. These peaks are more pronounced for larger amounts of OCTEO at the nanoparticle surface, which was also confirmed from the results of TGA, also reported before by Stauch *et al.* (Figure S4).[73] For all systems with silane modification, two main stages of weight loss were observed. The weight loss at low temperatures up to 250 °C is attributed to the evaporation of water physically adsorbed to the particle surface. The second weight loss region in the temperature range 250 °C – 900 °C results from the condensation of silanol groups to siloxane groups and the decomposition of organic moieties. Additionally, the weight loss of organic moieties increases with the amount of OCTEO. These measurements give a first insight to the extent of surface modification of the silica nanoparticles which will affect their surface properties.

To obtain further information especially on the behavior of the surface polarity, liquid tests were conducted (Figure S5). In a first test series, the modified nanoparticles were dispersed in water and toluene separately. Completely (1) and also partly modified (2/3, 1/2, 1/3, 1/5, 1/10) particles could not be dispersed well in water, but dispersed well in toluene (Figure S5a,b top row). This can be explained by the increase in hydrophobicity of the primary nanoparticles with increasing silane coverage and *vice versa*. After spray-drying of the nanoparticles, the effect becomes even more pronounced, since the hydrophobic nanostructured micro-raspberry particle powders float on the water surface whereas the hydrophilic particles enter water spontaneously (Figure S5a,b two middle rows). Subsequently, the particles were additionally treated with ultrasound to test the surface modification under mechanical stress (Figure S5a,b upper row). Particularly the micro-raspberries consisting of partly modified nanoparticles show differences compared to the picture obtained after having only shaken the samples. In

case of 1/3-modified nanoparticles, the powder can be partly dispersed in water, due to bursting of the micro-raspberries during ultrasonic treatment. This indicates that the individual nanoparticles apparently behave more hydrophilic than the micro-raspberry particles, which could be also seen from Figure S5a,b top row. In the case of 1/3-modification there should be 33 % octyl groups and 66 % silanol groups on the nanoparticle surfaces. The validity of the assumption that the silane modifies each individual nanoparticle to the same degree and *not* a fraction of nanoparticles completely and another fraction not at all, was confirmed in another, recent work.[74] Therein we transferred the modification principles to superparamagnetic particles with which we were able to clearly demonstrate that all nanoparticles are partly modified in the same way. As the details of this finding are very complex and as a repetition would be way too exhaustive in this current work, the reader is referred to this recent reference for a detailed information.[74] Therefore, the particles should show a more hydrophilic than hydrophobic behavior. In the case of the micro-raspberry particles the solid-liquid interface area (raspberry to solvent interface) is very small compared to individual nanoparticles (where liquid would need to cover every single nanoparticle surface). Therefore, the interaction of particle surfaces with liquid is significantly higher for nanoparticles after raspberries are broken upon sonication. Ultimately, the tendency in a rather amphiphilic system towards being either a tiny bit more hydrophilic or hydrophobic starts to matter. Thus, in the system here, the hydrophilic character is apparently slightly more pronounced. The result is that nanoparticles from bursted raspberry particles are obtained which tend to disperse slightly better in polar liquids.

To test the surface properties of the nanostructured micro-raspberry particles in more detail, in a second test series two-phase liquid tests based on an emulsification step were carried out (**Figure 1**). For this purpose, the particles were added to a toluene-water mixture and treated with an ultrasonic finger. It was observed that particles with average silane coverage of 1/2,

1/3 or 1/5 stabilize emulsions (Figure 1 b). To test the stability of these emulsions, the mixture was centrifuged. Only for samples consisting of 1/2-modified nanoparticles the emulsions were stable after centrifugation. This correlates well with the finding of Binks and Lumsdon who state that slightly hydrophobic/hydrophilic particles form more stable emulsions than strongly hydrophobic/hydrophilic particles.[12] Examination of the emulsion type reveals that the emulsion is water-in-oil (w/o). This finding also fits well with reports in the literature, according to which w/o emulsions are mostly formed by more hydrophobic particles (and herein, our particle system in the region of 2/3 to 1/3 modification turned out to have a slightly more pronounced tendency of hydrophobicity), whereas more hydrophilic particles prefer to stabilize o/w emulsions.[11,15]

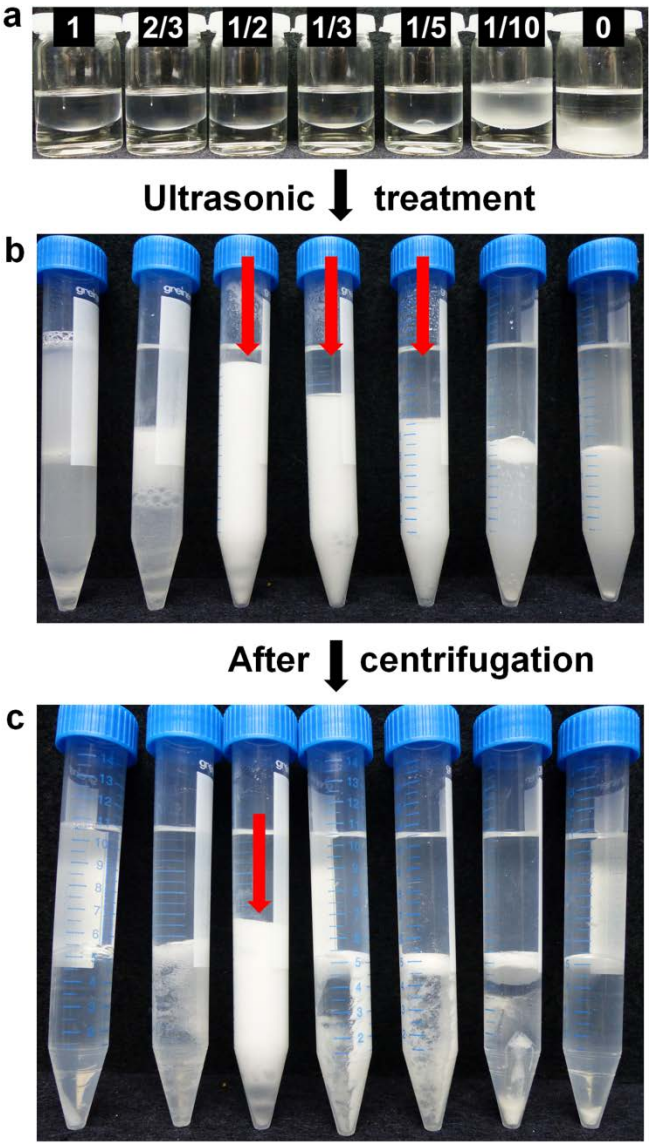

Figure 1. Nanostructured micro-raspberry powders (0.5 wt.-%) of SiO_2-NPs modified to different degrees with OCTEO: Completely modified (1), partly modified (2/3-modified, 1/2 modified, 1/3-modified, 1/5-modified, 1/10-modified) and non-modified (0) added to a two-phase system of water and toluene (a), after treatment with ultrasound (b) and after centrifugation (c). Emulsions of w/o are highlighted with red arrows.

Additionally, wettability tests with different water/methanol mixtures (0:100, 25:75, 50:50, 75:50, 100:0) were carried out to examine the surface polarity more precisely (Table S1, Figure S6). The wettability of all particle powders increases with increasing methanol content, whereby the particles with lower silane coverage could be wetted quicker. In pure methanol, the wettability of the particle samples modified to different degrees with silane is complete

and happens very quickly, while it takes days to wet partly hydrophobic particles in pure water. This behavior of silica particles modified with alkyl groups was also reported before by Li *et al.*[75] and Binks and Lumsdon.[12] In general, the more hydrophilic the particles are, the better is the wetting behavior into water/methanol. Noteworthy, this was confirmed for every water : methanol ratio.

Although the above experiments are only qualitative in nature, they provide very important information. As the behavior of all nanoparticles in each batch was the same, it can be qualitatively concluded that within a batch, at least globally, a high homogeneity is achieved. This means, in line with our recent findings,[74] that a partly modified system is exclusively composed of nanoparticles that are all partly modified and is not a mixture of fully and barely modified nanoparticles. However, determination of surface polarity of the nanostructured micro-raspberry particle system is quite challenging because of the various chemical groups on the particle surfaces. As already mentioned, there are approaches to examine the situation on a molecular level,[76] however this ultimate endeavor is very complex and challenging and thus clearly beyond the scope of this work.

Thus, so far it can only be stated that in the partly-modified case, a mixture of alkyl groups and also OH groups are located on the particle surfaces, which apparently lead to enhanced interface-activity of the particles. Obviously, the above experiments yield a quick visual impression of the behavior of the nanoparticles. However, it remains a purely phenomenological, thus qualitative observation. To pave the way for reliable predictions, quantitative results would be desirable to classify the polarity of particles. Thus, advanced techniques for quantification are needed and in the following the combination of HDP and RD methods are described.

3.3 Advanced methods

Determination of HDP

To get a better understanding of the surface modification, we carried out a HDP analysis as described in section 2.5 (for the calculated distance plot and the 2-D projections, the reader is referred to Figure S7 and our previous work[47]). In brief, the powders were dispersed in a set of defined liquids with known HSP (indicated by blue tetrahedra and red cubes in **Figure 2**) and measured by AC. Then, the measurements were evaluated resulting into an order of liquids, *i.e.* from the best to the poorest liquid as described above. It is based on an evaluation algorithm developed in our previous work where liquids are step-wise switched on, *i.e.*, ranked as good. By looking for the minimum "hop" of the HDP of the particles under investigation in 3D Hansen space as distinct point for the discrimination into "good" (*i.e.* blue tetrahedra) and "poor" (*i.e.* red cube), the 0/1-scoring into good liquids and poor liquids was obtained. The finally obtained HDP plot calculated *via* HSPiP (Hansen Solubility Parameters in Practice, 4th edition, version 4.1.07) software is exemplarily shown for non-modified micro-raspberry particles in Figure 2. The small blue tetrahedra inside and red cubes outside the green transparent dispersibility sphere indicate good and poor-ranked liquids, respectively. Its center represents the distinct HDP coordinates of non-modified nanostructured micro-raspberry particles. The three contributions of HDP and the radius of the sphere were determined to δ_D = 15.5 MPa$^{0.5}$, δ_P = 22.7 MPa$^{0.5}$, δ_H = 23.4 MPa$^{0.5}$ and R = 19.9 MPa$^{0.5}$.

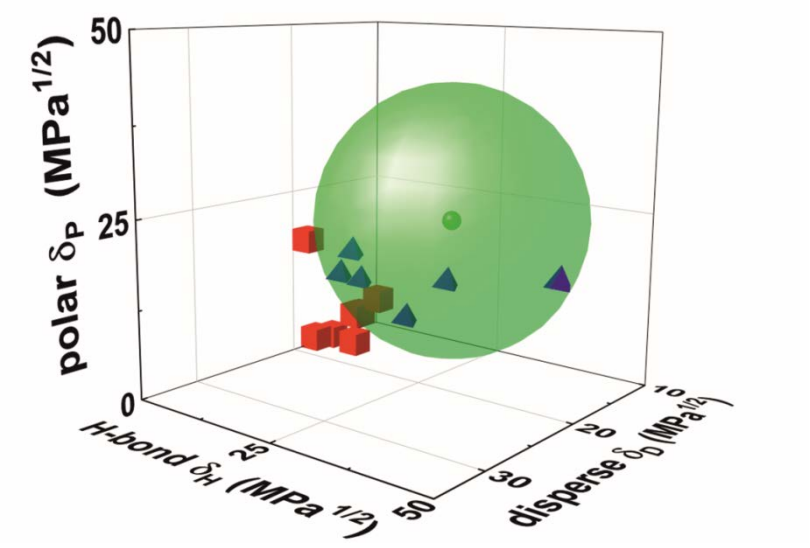

Figure 2. HDP sphere of non-modified nanostructured micro-raspberry particles derived from HSPiP software. The large green sphere indicates the dispersibility sphere of the particles with its distinct coordinates represented by the small green center in the middle. The blue triangles indicate the positions of good-ranked liquids whilst the red cubes indicate the positions of poor-ranked liquids.

In line with the structure and surface functionalities of the non-modified nanostructured micro-raspberry particles, a relatively low dispersion contribution and high polar and H-bond contributions were obtained, emanating from the hydrophilic Si-OH groups on native particle surfaces. Next, we investigated the differently OCTEO-modified nanostructured micro-raspberry particles. Already from the good ranked liquids it became clear that with the herein applied liquid list given in Table 1 three kinds of surfaces could be detected. For 0 and 1/10 surface modified raspberry particles, liquids 3, 6, 9, 10, 12, 13 were ranked good, for 1/5-2/3 surface modified raspberry particles liquids 3, 10, 12 and finally for 7/10-1 modified raspberry particles liquids 3, 5, 6, 9, 10, 12 were ranked good. Noteworthy, absolute relative sedimentation times (RSTs) which were derived using the integral extinction determined by AC,[47] did change gradually for every surface modification. However, due to the fact that the ranking, *i.e.* the order of good liquids sorted from the best to the worst liquid within regions I, II and III was constant, the resulting HDP did not change. Accordingly, **Figure 3** depicts the evolution of the individual HDP contributions, namely dispersion (Figure 3a), polar (Figure 3b) and H-bond (Figure 3c) with increasing silane coverage for regions I (0-1/10), II (1/5-2/3) and III (7/10-1). The dispersion contribution first increases followed by a plateau and then decreases starting from a silane coverage of 7/10. This is explained by the replacement of Si-OH groups by OCTEO molecules on the one hand, while at the same time additional carbon atoms are introduced. However, starting from a silane coverage of 7/10 to 1, the dispersion part of the OCTEO modified particles is quite low. This at first glance surprising evolution shows the complex interplay of ligand mixtures at particulate interfaces, which are for the

time being not sufficiently understood. Here we believe that quantification of such phenomena in combination with complementary solubility parameters like $E_T(30)$ and an in-depth understanding of the molecular level will shed light on these interesting effects. However, for the time being the latter would be far beyond the scope of this work which focuses on the quantification of particle surface properties rather than the in-depth understanding of the underlying molecular features.

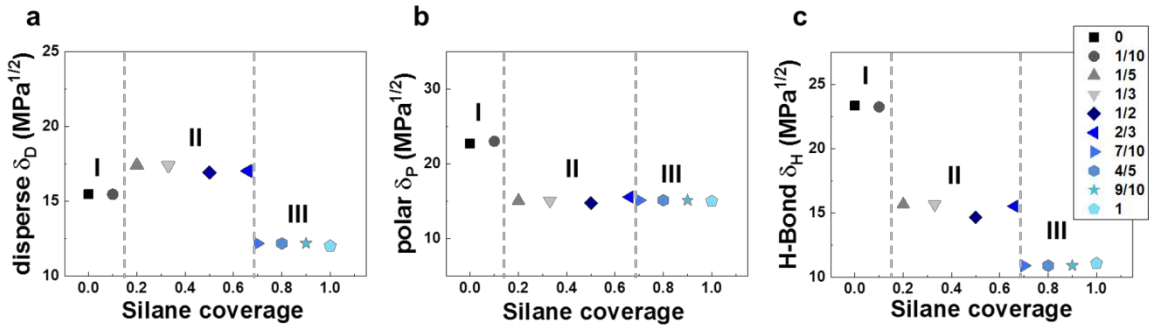

Figure 3. Evolution of single HDP contributions depending on OCTEO surface coverage of SiO_2-NPs. (a) δ_D, (b) δ_P, (c) δ_H.

Regarding δ_P and δ_H shown in Figure 3b and Figure 3c high values for both the polar and H-bond contributions for 0 and 1/10 modified particles are recognized. This is ascribed to the Si-OH groups at the surface, which are still dominant at 1/10 OCTEO coverage. Starting from 1/5 OCTEO coverage, the polar and H-bond contributions decrease, indicating the increasing influence of OCTEO that is replacing the OH groups on particle surface (Figure S8). Starting from 7/10 to full OCTEO coverage, the H-bond contribution steeply decreases while the polar contribution remains unchanged. Due to the replacement of Si-OH groups by OCTEO, more organic molecules are introduced and the particle surface becomes less polar. This leads to an overall decrease in the polar and H-bond contributions. Again, the reason why in region III the polar contribution is not affected, while the H-bond parameter is significantly reduced, cannot be explained without more detailed information of the molecules (re)organization at the molecular level.

Thus, from Figure 3 we can draw two conclusions. Firstly, we note that three major regions I-III are identified where we expect pronounced changes of HDP of the raspberry particles. Secondly, it becomes clear that for a more detailed resolution of the changes within I-III, a refinement of the liquid list in the regions of interest or an additional, complementary technique making the gradual changes accessible would be required. For instance, in future work, similar to the CST-approach of Boucher and Howell,[32] also the non-binary RST values as direct outcome of AC analysis could be processed.

Finally, we calculated the Hildebrand parameter δ as the sum of the single HDP contributions as reference quantity (note that in case of molecules δ would be the heat of evaporation relative to the molecular volume which is linked to the integral sum of all interactions, *i.e.*, not clearly defined in case of particles)[47]:

$$\delta = \sqrt{\delta_D^2 + \delta_P^2 + \delta_H^2} \qquad (4)$$

Noteworthy, the evolution of δ should follow the analogue trend as polarity as is depicted in the dependence of the silane coverage in **Figure** 4 (details on δ_i and R_i can be found in Table S2). As expected, firstly, δ is high in region I for non-modified and 1/10 modified nanostructured micro-raspberry particles, then decreases to a plateau in region II (1/5-2/3 modified samples) followed by a final noticeable decrease to region III with 7/10 to fully OCTEO modified micro-raspberry particles.

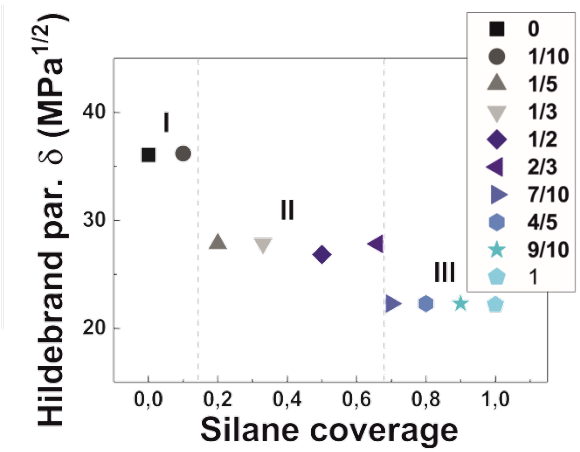

Figure 4. Evolution of the Hildebrandt parameter δ with silane coverage of SiO_2-NPs derived from the three HDP contributions.

Thus, our results show the strength of the HDP approach, as they quantitatively depict the decrease of polarity with increasing OCTEO coverage of surface-modified micro-raspberry particles. However, to better resolve the gradual change of the surface during OCTEO modification and for comparing HDP results with another independent and complementary method, RD studies were performed to investigate global polarity in more detail.

Reichardts's dye and comparison to HDP results

Reichardt's dye (RD) is a very useful indicator for the nature of silica particle surfaces,[69] thus it can be compared and correlated with the results from HDP. Other particle systems may

be explored with the method as well, although certainly not all as for instance in case of iron oxide nanoparticles the magnetic character would destroy the coloration of dyes due to quenching. The choice of suitable liquids for the adsorption process of the dye on the particle surfaces is very important. The solubility of RD is good in very polar liquids like methanol and therefore the dye molecules might not be completely adsorbed onto the silica particles. Depending on the adsorption-desorption equilibrium, most of them will remain in the liquid. To examine the influence of liquids on the $E_T(30)$ value of the silica particles in more detail, a slightly non-polar liquid, DCM, and the non-polar liquids *n*-octane and toluene were compared. In DCM, RD is highly soluble in contrast to *n*-octane where RD cannot be dissolved. Thus, in the latter solvent, the dye cannot be adsorbed on the silica surface. The reason is that for an adsorption process of the dye onto the nanoparticles, a minimum solubility in the liquid environment, *i.e.* in the solvent, has to be attained. In the case of DCM as liquid, RD could be adsorbed almost completely on the more hydrophilic micro-raspberry particles, whereas a residue of unbound dye remains in the supernatant after centrifugation of the more hydrophobic particles. In toluene, the affinity of RD towards going in solution is less pronounced. As a consequence, in this liquid, the driving force for RD adsorption onto the nanoparticle surfaces is enhanced. This can also be confirmed from visual inspection of the supernatant after the nanoparticles have been centrifuged following the adsorption process: What remains is a liquid which is hardly colored anymore. For this reason, toluene was chosen as the main liquid to conduct the dye adsorption on the silica nanoparticles.

The nanostructured micro-raspberry particle powders, modified to different degrees with silane, were therefore mixed with the RD-toluene solution to adsorb RD on the particle surfaces by the negatively charged oxygen atoms (**Figure 5**a). RD adsorbed on non-modified silica particle surfaces (0), appearing red, which becomes purple when adsorbed to partly-modified particles, and blue in the case of fully modified particles. These findings correlate

well with the findings from the liquid tests described above as well as with the HDP study, by which also three main regions were identified. As expected, the polarity degree of the particles decreases with increasing silane coverage. To calculate the $E_T(30)$ value of the particle samples as a quantitative measure for polarity, the $\pi \rightarrow \pi^*$ transition energy of the adsorbed dye was monitored by diffuse reflectance UV/Vis spectroscopy. For this purpose, the particles were carefully dried (Figure 5b). The colors of the adsorbed dye on the particle surfaces became brighter after drying and changed from red to orange for non-modified particle samples, from purple to pink for partly-modified particle samples and from blue to dark purple for fully modified particle samples. This is due to the absence of toluene. By visual inspection, the drying process seems to lead to a slight hypsochromic shift (blue shift), which means that the electronic ground state is better stabilized for dried particles than for particles dispersed in a non-polar liquid like toluene.

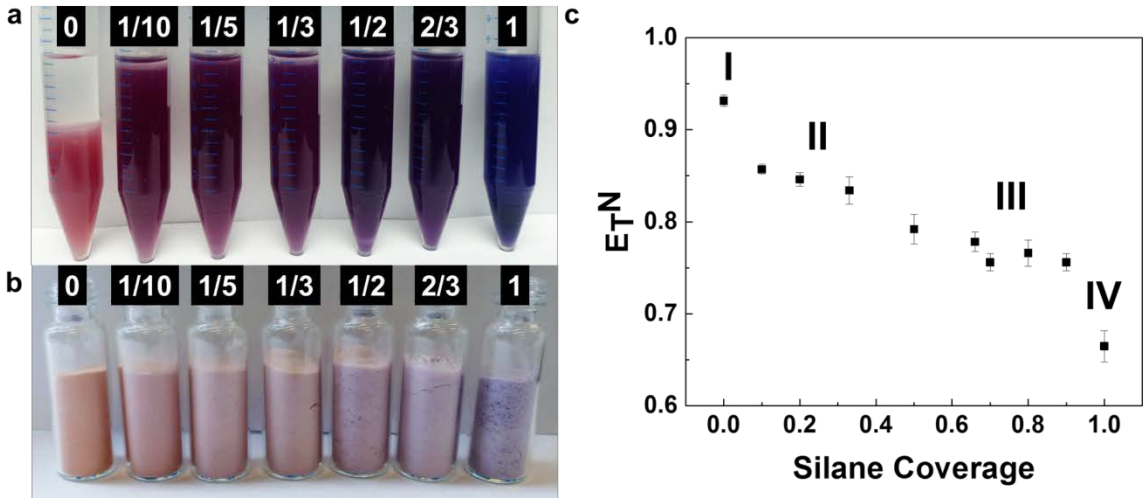

Figure 5. (a) Spray-dried SiO_2-NPs modified to different degrees with OCTEO (completely modified (1), partly modified (2/3-modified, 1/2 modified, 1/3-modified, 1/5-modified, 1/10-modified and non-modified (0)) dispersed in toluene containing RD. (b) Photos of above particle samples after drying in an oven. (c) Influence of the degree of OCTEO modification (1, 9/10, 8/10, 7/10, 2/3, 1/2, 1/3, 1/5, 1/10, 0) on the surface polarity parameter E_T^N determined by UV/Vis spectroscopy.

The calculated $E_T(30)$ values and E_T^N values decrease with increasing silane coverage of the nanoparticles (Table S3). A dependence of the $E_T(30)$ and E_T^N values on the original liquid the particles were dispersed in, can be excluded by comparing values for different liquids (toluene and DCM**,** Table S3) which indicates almost the same results. The E_T^N value of 0.93 for non-modified particles fits well with findings from the literature which report 0.96.[69,71,72] In contrast to HDP, four different regions could be observed: Two single point regions at the two extremes (unmodified (0) and completely modified (1) particles), a third region for slightly modified up to 1/3 modified particles and a fourth region for strongly modified (2/3 - 9/10) particles (Figure 5c). This trend could be attributed to the arrangement of the alkyl groups of the silane on the silica nanoparticle surface: We expected that small islands/patches of alkyl groups initially form, which grow with increasing amount of silane until the surface of a nanoparticle is completely covered with silane (Figure S9 depicts a scheme for this evolution). The RD is assumed to reach the silanol groups of the nanoparticles between the silane patches, yet with more patches / islands less dye can reach the surface. Noteworthy, this is in line with the expectations from HDP analysis. However, it should be also noted that the above interpretation is one possible explanation, but not necessarily the only potentially correct explanation. As can be seen in Figure 5c, also a somewhat linear trend could be attributed to the data points. It should further be noted that Figure S9 is only one model assumption and the reader should be careful in taking this model as “the real” situation. The point we would rather focus on is that only by quantitative analysis such discussions are enabled at all and potentially hand back questions to the molecular level. This is the reason why we think that the methods presented in this work are relevant in shedding light on surface properties on the particle level.

Finally, by comparing the E_T^N values with the values for mass loss between 250 and 900 °C against silane coverage, two different curve shapes were found (**Figure 6**). The curve of mass

loss is almost linear, throughout the E_T^N values decrease in four steps, which could be explained by the patchy like structure of the silane. Noteworthy, this finding clearly reveals that polarity of nanostructured micro-raspberry particles does not scale linearly with surface coverage but synergistic effects do occur. These were monitored by two completely independent techniques for characterization of surface properties, Hansen parameters and RD.

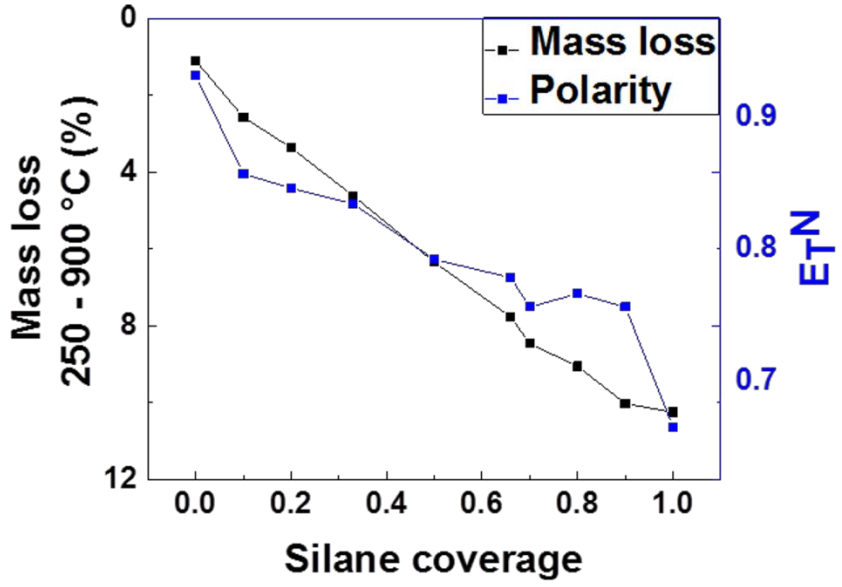

Figure 6. Variation of mass loss between 250 and 900 °C and E_T^N values *versus* silane coverage of spray-dried SiO_2-NPs.

4. Conclusion

Tailored surface properties of nanoparticles are of major importance for their subsequent processing in polymers to create polymer nanocomposites. A detailed understanding of the nanoparticle surface character is essential to obtain the desired dispersion results. Quick and simple dispersion tests in solvents and their subsequent inspection were demonstrated to be able to provide a first glimpse of the surface character of the particles. However, the current study went beyond and demonstrated that *via* more sophisticated analyses quantitative data

becomes accessible that can be compared throughout different laboratories. In fact, nanoparticle systems with a distinct degree of hydrophobicity or hydrophilicity, respectively, can be well resolved with respect to their surface character in a quantitative manner using Hansen parameters and Reichardt's dye characterization. Most importantly, our study revealed that surface properties in terms of e.g. polarity do not scale linearly with the amount of modification bound to the particle surface but synergistic effects clearly occur.

This is not only paving the way towards giving scientists a link for connecting particulate surface properties with the molecular level, but also gives to those who apply new functional (nano)particles in industrial products standardized characterization procedures, and thus strategies for quality control, at hand.

5. Experimental Section

Materials. Silica nanoparticles were used in aqueous dispersion at pH = 9.7 (Köstrosol 2040, K2040, Chemiewerke Bad Köstriz, Germany) containing 40 wt.% particles with a hydrodynamic diameter of 20 ± 2 nm (dynamic light scattering, Malvern Instruments Zeta Sizer, UK) without further purification. Octyltriethoxysilane (OCTEO, purity 97 %) for the modification of the silica nanoparticles and *n*-octane (purity 98 %) were purchased from abcr, Germany. Toluene (purity 99.8 %), methanol (MeOH, purity 99 %) and RD were purchased from Sigma-Aldrich, Germany and ethanol (EtOH, purity 99.5 %) was purchased from Jäcklechemie, Germany. Dichloromethane (DCM purity 99.9%) was purchased from Merck, Germany.

Modification of silica nanoparticles with OCTEO.[40] For the modification, 375 g deionized water (H_2O, conductivity 0.06 µS cm^{-1}) and 400 g ethanol (EtOH) was added within 15 min drop-wise and under stirring to 375 g silica sol K2040 (silica nanoparticles in water at pH = 9.7). Then, OCTEO was added as an ethanolic solution in the desired quantity. For a complete covering of particles with OCTEO, 45.5 g (164 mmol) were dissolved in 200 g EtOH, added

to the nanoparticle dispersion *via* a dropping funnel with stirring over 45 min. After combining the reactants, the reaction flask was refluxed at 78 °C for 3 h under stirring. Afterwards, the obtained dispersion was centrifuged (4301 RCA) for 60 min. Particles were washed thrice by re-dispersion in EtOH and subsequent centrifugation. To obtain partially silane-modified nanoparticles, the amount of silane was reduced to 2/3, 1/2, 1/3, 1/5, 1/10 of the amount above while the rest of the procedure remained unchanged.

Micro-raspberry synthesis.[40] To obtain nanostructured micro-raspberries, the (modified) nanoparticle dispersions were spray-dried in a B-290 mini spray dryer (Büchi, Switzerland). The inlet air temperature was set to 120 °C and the outlet temperature was 65–75 °C. Afterwards, the produced powders were dried in an oven at 110 °C for 48 h.

Liquid tests

Liquid tests. 50 mg of nanostructured micro-raspberry powder was mixed with either 10 g of toluene or 10 g of water and followed by shaking for a few minutes. Then, ultrasonic treatment for 5 min using an ultrasonic finger (Branson Sonifier 450, 400 W, Branson Ultrasonics, USA) was conducted with the following settings: Duty Cycle = 40, Output Control = 3.

Two-phase tests. 50 mg of nanostructured micro-raspberry powder was mixed with 5 g of toluene and 5 g of water. The mixture was treated with ultrasound for 20 min (4 x 5 min) using an ultrasonic finger (Branson Sonifier 450, 400 W, Branson Ultrasonics, USA) with the following settings: Duty Cycle = 40, Output Control = 3 with shaking in between and subsequently centrifugation at 7513 RCA for 8 min.

Wettability tests. 50 mg of micro-raspberry powder was placed on the surface of 10 ml of pure water, on the surface of mixtures (10 ml total) of water and methanol (75:25, 50:50, 25:75) and on the surface of 10 ml of methanol.

Hansen Dispersibility Parameter:

Liquids. All liquids used in this study including their abbreviations and dielectric constant ε are listed in Table 1. As described in our previous work,[47] liquids were selected in such way that their HSP coordinates allow a proper scanning of a wide range of the 3D Hansen space (**Figure S10**). In addition to the liquids used in our previous work, water was used as a probe liquid as silica nanoparticles are usually synthesized and stored in water.

Dispersion procedure. The spray-dried powder of micro-raspberry particles was used to prepare 0.01 wt.% dispersions in the respective liquids listed in Table 1. Afterwards, 15 min of ultrasound was applied to all suspensions using an ultrasonic bath at 20 °C (VWR International, 30 W according to the manufacturer). Then, samples were filled into measurement cells for AC analysis.

AC analysis. All AC measurements were carried out with a LUMiSizer LS 651 (LUM GmbH, Germany) using the blue wavelength (470 nm) to maximize the signal of small particles with low scattering intensity. The set temperature of all measurements was 20 °C. Polyamide measurement cells with an optical path length of 2 mm (LUM GmbH, Germany) were used as received and filled with 430 µl of suspension. After ultrasonic treatment, the cells were inserted immediately to the rotor and centrifugation was performed with no delay at 500 rpm corresponding to a relative centrifugal acceleration (RCA) of 36 at the cell bottom.

Table 1. Liquids used for HDP determination.

Liquid	E	Purity/%	Supplier
1. n-hexane (Hex)	1.9	≥ 95	C. Roth, Germany
2. Toluene (Tol)	2.4	≥ 99.5	C. Roth, Germany
3. n-methyl-2-pyrrolidone (NMP)	32.6	≥ 99.8	C. Roth, Germany
4. 1,4-dioxane (Diox)	2.2	≥ 99.5	C. Roth, Germany
5. Ethyl acetate (EA)	6.1	> 99.5	C. Roth, Germany
6. Acetone (Act)	21.0	≥ 99.8	C. Roth, Germany
7. Diacetone alcohol (DAA)	18.2	≥ 98	Merck, Germany
8. Tetrahydrofuran (THF)	7.5	≥ 99.5	C. Roth, Germany
9. Isopropyl alcohol (IPA)	20.2	≥ 99.8	C. Roth, Germany
10. Dimethyl sulfoxide (DMSO)	27.2	≥ 99.5	C. Roth, Germany
11. Propylene carbonate (PC)	66.1	≥ 99.7	C. Roth, Germany
12. Methanol (MeOH)	33.0	≥ 99.9	C. Roth, Germany
13. Millipore water (H_2O)	80.1		

HDP evaluation. Since the general method of HDP derivation using our AC approach is already described in our previous work, we will only give a brief summary. For the detailed procedure, the reader is referred to literature.[47] In order to determine HDP, the stability of particles, *i.e.* the presence/absence of agglomeration/flocculation has to be evaluated in a defined set of probe liquids. Afterwards, samples have to be classified into so-called “good” and “poor” ones to get a liquid ranking from the best to the worst. To visualize stability in an objective way, we monitored the sedimentation behaviour in an AC experiment which is - in brief - a sedimentation experiment with optical access in time and space. As larger

agglomerates/flocs sediment faster compared to smaller ones, the sedimentation time (t_{sed}) of particles in different liquids, which can be derived from the integral extinction as measurement quantity, is a measure of their stability against agglomeration/flocculation. From t_{sed}, the so-called relative sedimentation time (RST) is derived after considering the density difference between the particle (ρ_P) and the liquid (ρ_L), the liquid viscosity (η_L), the centrifugal acceleration (a) and the optical path length of the cuvette (d_{cell}):

$$RST = \frac{t_{sed}(\rho_P - \rho_{L,i})a}{\eta_{L,i} d_{cell}} \quad (3)$$

By comparing RST values in different probe liquids, a ranking from the best (largest RST) to the worst (smallest RST) liquid can be established. Then, using an evaluation algorithm developed by us where the number of good ranked liquids is stepwise increased according to the RST ranking, a well-defined HDP for a given material is obtained in an objective way. For more details on the standardized derivation of HDP by AC, the reader is referred to Süß *et al.*[47]

Preparation of micro-raspberry particles with RD. 10 mg of RD was dissolved in 10 g of toluene or DCM and mixed with a vortex (Vortex 4 basic, IKA, Germany). Subsequently, 1.5 g of nanostructured micro-raspberry particle powder with different surface modification was added to 3.75 g of toluene/DCM-dye mixture (amount of dye: 4.5 µmol/g). The suspension was mixed for 5 min in a rotary evaporator and centrifuged at 7513 RCA for 10 min. The supernatant was discarded and the particles were dried in an oven at 60 °C and 60 bar for 48 h.

Analyses. Scanning electron microscopy (SEM) was carried out with a Zeiss Supra 25 SEM at an acceleration voltage of 3 keV. The micro-raspberry powders were placed on a SEM sample

holder equipped with a sticky carbon pad without further treatment. Differential thermogravimetric analysis (TGA) was carried out starting from 30 °C up to 900 °C (heating rate = 10 K min^{-1}) with a TG 209 F1 Libra DTA-TG (Netzsch, Germany). Fourier-transform infrared spectroscopy (FTIR, Nicolet MagnaIR 760 Spectrometer E.S.P., USA) was used to analyze the silica particles in KBr pellets. UV/Vis Spectroscopy was performed using a Shimadzu UV3100 instrument (Nakagyoku, Japan). The spectrum of the solids was measured against $BaSO_4$ in a diffuse reflectance mode.

Supporting Information

Supporting Information is available from the Wiley Online Library or from the author.

Acknowledgement

This work was supported by the Fraunhofer Internal Programs under Grant No. MAVO 828 483. DS and SS acknowledge the funding of Deutsche Forschungsgemeinschaft (DFG) through the Cluster of Excellence “Engineering of Advanced Materials”. Moreover, we thank the Federal Ministry of Economic Affairs through the Arbeitsgemeinschaft industrieller Forschungsvereinigungen “Otto von Guericke” e.V. (AiF, project no. KF 2347922UW4). Furthermore, we thank Prof. Steven Abbott and Dr. Charles M. Hansen for a license of HSPiP software.

Received: ((will be filled in by the editorial staff))
Revised: ((will be filled in by the editorial staff))
Published online: ((will be filled in by the editorial staff))

References

[1] G. Chen, S. Zhou, G. Gu, H. Yang, L. Wu, *J. Colloid Interface Sci.* **2005**, 281, 339.

[2] S. Kango, S. Kalia, A. Celli, J. Njuguna, Y. Habibi, R. Kumar, *Prog. Polym. Sci.* **2013**, 38, 1232.

[3] A. Bouty, L. Petitjean, C. Degrandcourt, J. Gummel, P. Kwaśniewski, F. Meneau, F. Boué, M. Couty, J. Jestin, *Macromolecules* **2014**, 47, 5365.

[4] G. Chen, S. Zhou, G. Gu, L. Wu, *Colloids Surf., A* **2007**, 296, 29.

[5] R. Y. Hong, H. P. Fu, Y. J. Zhang, L. Liu, J. Wang, H. Z. Li, Y. Zheng, *J. Appl. Polym. Sci.* **2007**, 105, 2176.

[6] O. D. Velev, K. Furusawa, K. Nagayama, *Langmuir* **1996**, 12, 2374.

[7] F. Leal-Calderon, V. Schmitt, *Curr. Opin. Colloid Interface Sci.* **2008**, 13, 217.

[8] T. S. Horozov, B. P. Binks, *Angew. Chem. Int. Ed.* **2006**, 45, 773.

[9] R. Aveyard, B. P. Binks, J. H. Clint, *Adv. Colloid Interface Sci.* **2003**, 100-102, 503.

[10] B. P. Binks, S. O. Lumsdon, *Phys. Chem. Chem. Phys.* **1999**, 1, 3007.

[11] B. P. Binks, S. O. Lumsdon, *Langmuir* **2000**, 16, 2539.

[12] B. P. Binks, S. O. Lumsdon, *Langmuir* **2000**, 16, 8622.

[13] B. P. Binks, *Curr. Opin. Colloid Interface Sci.* **2002**, 7, 21.

[14] B. P. Binks, C. P. Whitby, *Colloids Surf., A* **2005**, 253, 105.

[15] P. Finkle, H. D. Draper, J. H. Hildebrand, *J. Am. Chem. Soc.* **1923**, 45, 2780.

[16] A. Hasan, L. M. Pandey, *Mat. Sci. Eng. C* **2016**, 68, 423.

[17] R. M. Pasternack, S. Rivillon Amy, Y. J. Chabal, *Langmuir* **2008**, 24, 12963.

[18] W. Lin, J. Walter, A. Burger, H. Maid, A. Hirsch, W. Peukert, D. Segets, *Chem. Mater.* **2014**, 27, 358.

[19] J. Mijatovic, W. H. Binder, H. Gruber, *Microchim. Acta* **2000**, 133, 175.

[20] J. de Roo, S. Coucke, H. Rijckaert, K. de Keukeleere, D. Sinnaeve, Z. Hens, J. C. Martins, I. van Driessche, *Langmuir* **2016**, 32, 1962.

[21] J. de Roo, I. van Driessche, J. C. Martins, Z. Hens, *Nat. Mater.* **2016**, 15, 517.

[22] W. J. Malfait, S. Zhao, R. Verel, S. Iswar, D. Rentsch, R. Fener, Y. Zhang, B. Milow, M. M. Koebel, *Chem. Mater.* **2015**, 27, 6737.

[23] J. de Roo, N. Yazdani, E. Drijvers, A. Lauria, J. Maes, I. van Driessche, M. Niederberger, V. Wood, J. C. Martins, I. Infante, Z. Hens, *ChemRxiv*, **2018**.

[24] M. Valentini, A. Vaccaro, A. Rehor, A. Napoli, J. A. Hubbell, N. Tirelli, *J. Am. Chem. Soc.* **2004**, 126, 2142.

[25] T. Schindler, T. Schmutzler, M. Schmiele, W. Lin, D. Segets, W. Peukert, M.-S. Appavou, A. Kriele, R. Gilles, T. Unruh, *J. Colloid Interface Sci.* **2017**, 504, 356.

[26] D. Sriramulu, E. L. Reed, M. Annamalai, T. V. Venkatesan, S. Valiyaveettil, *Sci. Rep.* **2016**, 6, 35993.

[27] C. H. Lee, S. H. Park, W. Chung, J. Y. Kim, S. H. Kim, *Colloids Surf., A* **2011**, 384, 318.

[28] S. Park, J. An, I. Jung, R. D. Piner, S. J. An, X. Li, A. Velamakanni, R. S. Ruoff, *Nano letters* **2009**, 9, 1593.

[29] L. Vaisman, H. D. Wagner, G. Marom, *Advances in Colloid and Interface Science* **2006**, 128-130, 37.

[30] F. Machui, S. Langner, X. Zhu, S. Abbott, C. J. Brabec, *Sol. Energy Mater. Sol. Cells* **2012**, 100, 138.

[31] M. Roesing, J. Howell, D. Boucher, *J. Polym. Sci. Part B: Polym. Phys.* **2017**, 55, 1075.

[32] D. Boucher, J. Howell, *J. Phys. Chem. B*, **2016**, 120, 11556.

[33] G. Grause, S. Hirahashi, H. Toyoda, T. Kameda, T. Yoshioka, *J. Mater. Cycles Waste Manag.* **2017**, 19, 612.

[34] C. E. Johnson, M. P. Gordon, D. S. Boucher, *J. Polym. Sci. Part B: Polym. Phys.* **2015**, 53, 841.

[35] Y. Lan, M. G. Corradini, R. G. Weiss, S. R. Raghavan, M. A. Rogers, *Chem. Soc. Rev.* **2015**, 44, 6035.

[36] Y. Lan, M. G. Corradini, X. Liu, T. E. May, F. Borondics, R. G. Weiss, M. A. Rogers, *Langmuir* **2014**, 30, 14128.

[37] N. Yan, Z. Xu, K. K. Diehn, S. R. Raghavan, Y. Fang, R. G. Weiss, *J. Am. Chem. Soc.* **2013**, 135, 8989.

[38] L. P. Novaki, E. O. Moraes, A. B. Gonçalves, R. A. de Lira, V. N. Linhares, M. C. K. de Oliveira, F. A. Meireles, G. Gonzalez, O. A. El Seoud, *Energy Fuels* **2016**, 30, 4644.

[39] L. P. Novaki, R. Lira, M. M. N. Kwon, M. C. K. de Oliveira, F. A. Meireles, G. Gonzalez, O. A. El Seoud, *Energy Fuels* **2018**, 32, 3281.

[40] C. Stauch, T. Ballweg, W. Stracke, R. Luxenhofer, K. Mandel, *J. Colloid Interface Sci.* **2017**, 490, 401.

[41] S. Gårdebjer, M. Andersson, J. Engström, P. Restorp, M. Persson, A. Larsson, *Polym. Chem.* **2016**, 7, 1756.

[42] C. Backes, N. C. Berner, X. Chen, P. Lafargue, P. LaPlace, M. Freeley, G. S. Duesberg, J. N. Coleman, A. R. McDonald, *Angew. Chem. Int. Ed.* **2015**, 54, 2638.

[43] J. N. Coleman, *Adv. Funct. Mater.* **2009**, 19, 3680.

[44] J. M. Hughes, D. Aherne, J. N. Coleman, *J. Appl. Polym. Sci.* **2013**, 127, 4483.

[45] D. Lerche, S. Horvat, T. Sobisch, *Dispersion Lett.* **2015**, 6, 13.

[46] J. B. Petersen, J. Meruga, J. S. Randle, W. M. Cross, J. J. Kellar, *Langmuir* **2014**, 30, 15514.

[47] S. Süß, T. Sobisch, W. Peukert, D. Lerche, D. Segets, *Adv. Powder Technol.* **2018**, 29, 1550.

[48] K.-C. Choi, E.-J. Lee, Y.-K. Baek, M.-J. Kim, Y.-D. Kim, P.-W. Shin, Y.-K. Kim, *RSC Adv.* **2014**, 4, 7160.

[49] H. T. Ham, Y. S. Choi, I. J. Chung, *J. Colloid Interface Sci.* **2005**, 286, 216.

[50] K. Maleski, V. N. Mochalin, Y. Gogotsi, *Chem. Mater.* **2017**, 29, 1632.

[51] L. M. Wheeler, N. J. Kramer, U. R. Kortshagen, *Nano letters* **2018**, 18, 1888.

[52] w. H.-S. com. Similarity | Hansen Solubility Parameters. https://www.hansen-solubility.com/HSP-science/Similarity.php (accessed July 30, 2018).

[53] w. H.-S. com. HSP Examples: Measuring Nanoparticles | Hansen Solubility Parameters. https://www.hansen-solubility.com/HSP-examples/measure-nanoparticles.php (accessed July 30, 2018).

[54] M. A. Boles, D. Ling, T. Hyeon, D. V. Talapin, *Nat. Mater.* **2016**, 15, 141.

[55] B. Fritzinger, I. Moreels, P. Lommens, R. Koole, Z. Hens, J. C. Martins, *J. Am. Chem. Soc.* **2009**, 131, 3024.

[56] N. H. Moreira, A. Domıinguez, T. Frauenheim, A. L. da Rosa, *Phys. Chem. Chem. Phys.* **2012**, 14, 15445.

[57] M. C. S. Pierre, P. M. Mackie, M. Roca, A. J. Haes, *J. Phys. Chem. C* **2011**, 115, 18511.

[58] G. Ramakrishna, H. N. Ghosh, *Langmuir* **2003**, 19, 3006.

[59] S. Saha, P. Sarkar, *RSC Adv.* **2014**, 4, 1640.

[60] M. Zobel, A. Windmüller, E. M. Schmidt, K. Götz, T. Milek, D. Zahn, S. A. J. Kimber, J. M. Hudspeth, R. B. Neder, *CrystEngComm.* **2016**, 18, 2163.

[61] S. Dash, S. Mishra, S. Patel, Mishra, K., Bijay, *Adv. Colloid Interface Sci.* **2008**, 140, 77.

[62] J. L. Jones, S. C. Rutan, *Anal. Chem.* **1991**, 63, 1318.

[63] S. Nigam, S. Rutan, *Appl. Spectrosc.* **2016**, 55, 362–370.

[64] Y. Zimmermann, S. Spange, *J. Phys. Chem. B* **2002**, 106, 12524.

[65] W. Tian, J. Tian, *Dyes Pigm.* **2014**, 105, 66.

[66] A. Abdollahi, Z. Alinejad, A. R. Mahdavian, *J. Mater. Chem. C* **2017**, 5, 6588.

[67] C. Reichardt, *Chem. Rev.* **1994**, 94, 2319.

[68] D. Crowther, X. Liu, *J. Chem. Soc. Chem. Commun.* **1995**, 2445.

[69] D. J. Macquarrie, S. J. Tavener, G. W. Gray, P. A. Heath, J. S. Rafelt, S. I. Saulzet, J. J. E. Hardy, J. H. Clark, P. Sutra, D. Brunel, F. di Renzo, F. Fajula, *New J. Chem.* **1999**, 23, 725.

[70] B. Onida, S. Fiorilli, L. Borello, G. Viscardi, D. Macquarrie, E. Garrone, *J. Phys. Chem. B* **2004**, 108, 16617.

[71] S. Spange, A. Reuter, D. Lubda, *Langmuir* **1999**, 15, 2103.

[72] S. J. Tavener, J. H. Clark, G. W. Gray, P. A. Heath, D. J. Macquarrie, *Chem. Commun.* **1997**, 1147.

[73] C. Stauch, T. Ballweg, K.-H. Haas, R. Jaeger, S. Stiller, A. Shmeliov, V. Nicolosi, S. Malebennur, J. Wötzel, M. Beiner, R. Luxenhofer, K. Mandel, *Polym. Compos.* **2018**, 48, 410.

[74] C. Stauch, S. Späth, T. Ballweg, R. Luxenhofer, K. Mandel, *J. Colloid Interface Sci.* **2017**, 505, 605.

[75] Li, Z., Rutan, S. C., Dong, S., *Anal. Chem.* **1996**, 68, 124.

[76] W. Lin, J. Walter, A. Burger, H. Maid, A. Hirsch, W. Peukert, D. Segets, *Chem. Mater.* **2014**, 27, 358.

The quantitative determination of surface polarity properties of nanoparticles is achieved *via* the combination of analytical centrifugation and subsequent deduction of Hansen parameters with Reichardt`s indicator data.

Keyword: colloidal stability, silica particles, interface characterization, surface coating, analytical centrifugation

Claudia Stauch, Sebastian Süß, Robert Luxenhofer, Bernard P. Binks, Doris Segets* and Karl Mandel*

Quantifying surface properties of silica particles by combining Hansen parameters and Reichardt's dye indicator data